CHARACTERIZATION OF PULMONARY ARTERIAL BRANCHING IN RAT FETUSES WITH CONGENITAL DIAPHRAGMATIC HERNIA

by

Furkan Durmuş

B.S., in Biomedical Engineering, Erciyes University, 2016

Submitted to the Institute of Biomedical Engineering
in partial fulfillment of the requirements
for the degree of
Master of Science
in
Biomedical Engineering

Boğaziçi University
2020

CHARACTERIZATION OF PULMONARY ARTERIAL BRANCHING IN RAT FETUSES WITH CONGENITAL DIAPHRAGMATIC HERNIA

APPROVED BY:

Assoc. Prof. Dr. Esin Öztürk Işık .....
(Thesis Advisor)

Dr. Bora Büyüksaraç .....
(Thesis Co-advisor)

Dr. Emrah Aydın .....

Dr. Daniela Schults .....

Assoc. Prof. Dr. Duygu Ege .....

DATE OF APPROVAL: 15.09.2020

ACKNOWLEDGMENTS

First of all, I would like to express my gratitude to my thesis supervisor, Assoc. Prof. Dr. Esin Öztürk Işık, who was very patient and helpful throughout my graduate studies. She always encouraged me and helped me increase my motivation. Additionally, I would like to thank Asst. Prof. Dr. Emrah Aydın, who has never withheld his help for this thesis study. I also would like thank my family for their support and patience.

ACADEMIC ETHICS AND INTEGRITY STATEMENT

I, Furkan Durmuş, hereby certify that I am aware of the Academic Ethics and Integrity Policy issued by the Council of Higher Education (YÖK) and I fully acknowledge all the consequences due to its violation by plagiarism or any other way.

Name :

Signature:

Date:

ABSTRACT

CHARACTERIZATION OF PULMONARY ARTERIAL BRANCHING IN RAT FETUSES WITH CONGENITAL DIAPHRAGMATIC HERNIA

Congenital diaphragmatic hernia (CDH) is one of the congenital anomalies leading to neonatal deaths and postnatal respiratory disorders. When the abdominal organs herniate into the chest through the defect on the diaphragm, pulmonary hypoplasia and pulmonary hypertension might occur. Pulmonary hypoplasia is defined as the underdevelopment of the lung. On the other hand, pulmonary hypertension is defined as the increased pressure applied to the pulmonary artery wall due to the structural changes of the arteries. During the fetal period, the fetus gets oxygen through the placenta instead of using its own lungs. Although the pathology starts in utero, the pressure levels in the respiratory system could be measured postnatally. Even there are studies in the literature that aims to predict the severity of the disease in utero, none of them widely accepted. The methods used to estimate the degree of CDH include lung-to-head ratio, total lung volume, and the presence of a liver hernia. In this study, the data of rat fetuses gathered via micro-computed tomography (μCT) were employed to compute the morphometric measurements of the pulmonary arteries and evaluated to predict the outcome of CDH. In future studies, new methods could be developed to assess the degree of the CDH anomaly in utero to help doctors with a surgical intervention decision.

Keywords: Congenital diaphragmatic hernia, pulmonary hypertension, pulmonary hypoplasia, vessel segmentation, micro computed tomography (μCT).

ÖZET

KONJENİTAL DİYAFRAM HERNİLİ SIÇAN FETÜSLERİNDE AKCİĞER ATARDAMARI DALLANMASININ KARAKTERİZASYONU

Konjenital diyafragma herni (KDH), neonatal ölümlere ve doğum sonrası solunum bozukluklarına yol açan konjenital anomalilerden biridir. Karın organları diyaframdaki defekt yoluyla göğse fıtıklaştığında, pulmoner hipoplazi ve pulmoner hipertansiyon oluşabilir. Pulmoner hipoplazi, akciğerin yetersiz gelişmesi olarak tanımlanır. Pulmoner hipertansiyon ise arterlerdeki yapısal değişiklikler nedeniyle pulmoner arter duvarına uygulanan basınç artışı olarak tanımlanır. Fetal dönemde fetüs, kendi solunum sistemini kullanmak yerine plasentadan oksijen alır. Patoloji uterusta başlamasına rağmen solunum sistemindeki basınç seviyesi doğum sonrası dönemde ölçülebilmektedir. Literatürde hastalığın derecesini uterusta tahmin etmeyi amaçlayan çalışmalar olsa da hiçbiri geniş kabul görmemektedir. KDH'ın derecesini tahmin etmek için kullanılan yöntemler arasında akciğer-kafa oranı, toplam akciğer hacmi ve karaciğerin fıtıklaşması gibi parametreler sayılabilir. Bu çalışmada, mikro-bilgisayarlı tomografi (μBT) ile toplanan sıçan fetüslerinin verileri, pulmoner arterlerin morfometrik ölçümlerini hesaplamak için kullanılmış ve KDH'ın sonucunu tahmin etmek için değerlendirilmiştir. Gelecekteki çalışmalarda, doktorlara cerrahi müdahaleye karar mekanizmasında yardımcı olmak ve KDH anomalisinin derecesini değerlendirmek için yeni yöntemler geliştirilebilir.

Anahtar Sözcükler: Konjenital diyafram hernisi, pulmoner hipertansiyon, pulmoner hipoplazi, damar segmentasyonu, mikro bilgisayarlı tomografi (μBT).

TABLE OF CONTENTS

LIST OF FIGURES

LIST OF TABLES

LIST OF ABBREVIATIONS

μCT	Micro-Computed Tomography
CDH	Congenital Diaphragmatic Hernia
DICOM	Digital Imaging and Communications in Medicine
ECMO	Extracorporeal Membrane Oxygenation
TO	Tracheal Occlusion
HASTE	Half-Fourier Acquisition Turbo Spin Echo
LDR	Length to Diameter Ratio
LHR	Lung Area to Head Circumference Ratio
MRI	Magnetic Resonance Imaging
RF	Radio Frequency
SSFSE	Single-Shot Fast-Spin Echo

1. INTRODUCTION

Congenital diaphragmatic hernia (CDH), a defect that occurs during the formation of the diaphragm, has a major effect on the ratio of dead born. Subsequent pulmonary diseases, such as pulmonary hypoplasia and pulmonary hypertension, are possible outcomes of this defect. Determining the severity of the CDH is crucial to decide whether to intervene with the fetus. There have been some non-invasive methods proposed to determine the severity of the CDH during the fetal period, such as measuring the ratio of the lung diameter to thoracic circumference [8], left/right ventricle ratio [9], lung volume to body weight ratio [10], lung area to head circumference ratio (LHR) [11, 12], the presence of polyhydramnios [13], and position of the liver [14] using imaging techniques. While pulmonary hypoplasia could be predicted by these techniques and the severity of the outcomes could be reduced by surgical interventions such as tracheal occlusion [15], pulmonary hypertension could not be detected by non-invasive methods during the fetal period. There has also been a debate on whether these parameters precisely predict the mortality rate or not [16].

In the literature, some parameters including the total lung volume, the ratio of right and left ventricles, and lung to head ratio, have been used to evaluate the effects of CDH in humans. On animal subjects, these ratios have not been taken into consideration, but histological measurements were made. At present, the only way to detect the severity of pulmonary hypertension is histologic studies on postmortem subjects which showed that pulmonary hypertension results in a lower number of arterial branches and an increase in the mean vessel wall thickness [17, 18]. A cure for pulmonary hypertension due to CDH is not yet available. However, early detection of the severity of pulmonary hypertension and subsequent intervention to the fetus may help with reducing postnatal morbidity. For example, extracorporeal membrane oxygenation (ECMO) is a method that oxygenates and cleans the blood outside of the body and returns it to the heart, and it could be applied to newborns, who have respiratory disorders. The clinical studies have shown that this method effectively lowers the mor-

bidity rate when applied to neonates with high CDH severity [19]. So, it is important to assess the vessel network and intervene with the fetus whenever necessary.

In order to perform morphometric measurements precisely in the fetal period, Aydın et al. [20] developed a new pulmonary vasculature imaging method in rat fetuses as a preliminary study. This follow-up thesis study aims to characterize the pulmonary vasculature and evaluate the morphometric measurements of the rat subjects to establish new prognostic predictors of CDH severity utilizing non-invasive imaging methods.

2. BACKGROUND

2.1 Fetal Circulation

In mammals, the blood circulation system has significant differences between prenatal and postnatal periods [21]. Since the lungs of the fetus will be active after birth, the oxygenation of the blood is supplied through the placenta through the umbilical cord. The oxygenated blood passes through the liver of the fetus with the umbilical vein and enters the vena cava and then goes to the right atrium. Due to the resistance in the fluid-filled lung, high pressure occurs in the right atrium of the heart. Because of this pressure, some of the blood passes from the right atrium to the left atrium via the hole in the foramen ovale and some passes to the right ventricle. A small amount of blood passes into the right ventricle and the lung through the pulmonary artery to feed the lung. At this time, pressure on the pulmonary arteries gets too high. The blood passing from the left atrium to the left ventricle passes to the aorta. Normally, the contaminated blood in the right ventricle is sent to the lung through the pulmonary artery to be oxygenated, in the fetus the blood that mixed in the foramen oval is sent to the placenta to be oxygenated by passing it to the umbilical artery by passing through the ductus arteriosus [22]. After birth, foramen ovale, ductus venosus, and ductus arteriosus disappear and normal blood circulation starts.

In this study, we analyzed rat subjects. There are some anatomical and physiological differences between rat and human pulmonary systems. The lungs of rats and humans are divided into two parts as the right and left lungs (Figure 2.1). While the left lung of the rats consists of one lobe, the left lung of humans consists of two lobes. On the other hand, the right lung of the rats consists of 4 lobes, and the right lung of the humans consists of 3 lobes. The lobes are separated by the lobar fissures. Despite the differences in lung structures, there is not a big difference between the lung bronchial formation and functions of the rat and human lungs [23].

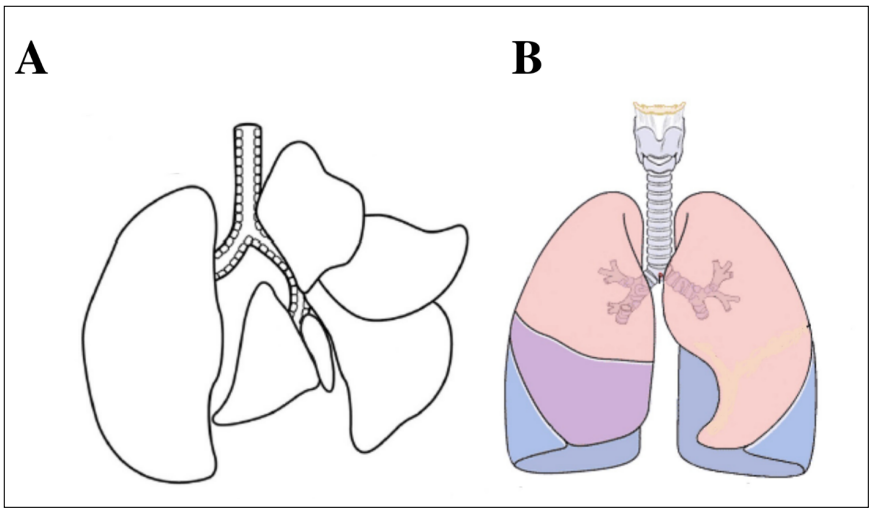

Figure 2.1 A: Lung anatomy of a rat [1], B: Lung anatomy of a human [2].

2.2 Congenital Diaphragmatic Hernia

The transient pleuroperitoneal fold arises from the posterior body wall and appears in late-week 4 and is present until week 6. After this time, it can no longer be separated from the diaphragm. The diaphragm completes its formation around the 12th week of gestation. If diaphragmatic muscle fails to close between 6-10th weeks of gestation, abdominal organs may herniate into the chest cavity through the defect resulting in the congenital diaphragmatic hernia (CDH). The defect happens either posterolaterally, so-called Bochdalek Hernia, or anteriorly so-called Morgagni Hernia. Bochdalek hernia is more common and has a poorer prognosis when compared to Morgagni Hernia which is mostly diagnosed incidentally. Therefore, CDH mostly refers to Bochdalek Hernia unless otherwise indicated. The exact cause of this anomaly has not been identified yet. However, some genetic factors have been identified as dominant factors of CDH [24]. To detect CDH anomaly, experts check for the polyhydramnios, liver herniation, abdominal organ herniations, and lung-to-head ratio (LHR) [25]. Even though the improvements in medical science makes detecting the CDH easier and improve the survival rates of the infants, it is still one of the most prominent diseases that cause high mortality in the newborns [26]. Abdominal organs may herniate to the upper side of the chest from this hernia and cause dislocation of the thoracic structures

(Figure 2.2). While usually, it occurs on the left side, it is possible to occur on the right side of the hernia or bilaterally [27]. This phenomenon results in the underdevelopment of the lungs as well as an increase in the thickness of the muscular layer of the pulmonary arterioles, hence the outcome is pulmonary hypoplasia and pulmonary hypertension in the newborn. Besides, polyhydramnios, which is excessive accumulation of the amniotic fluid, could be observed, which makes the pregnancy period more complicated. Polyhydramnios and pulmonary hypoplasia could be detected by ultrasound imaging [28]. Since the fetal blood circulation limits the blood flow to the lungs [29], pulmonary hypertension could not be demonstrated by conventional methods, but could only be measured by non-invasive methods after birth. As a result of the underdevelopment of the lungs, there would be decreased airway branching and alveolarization.

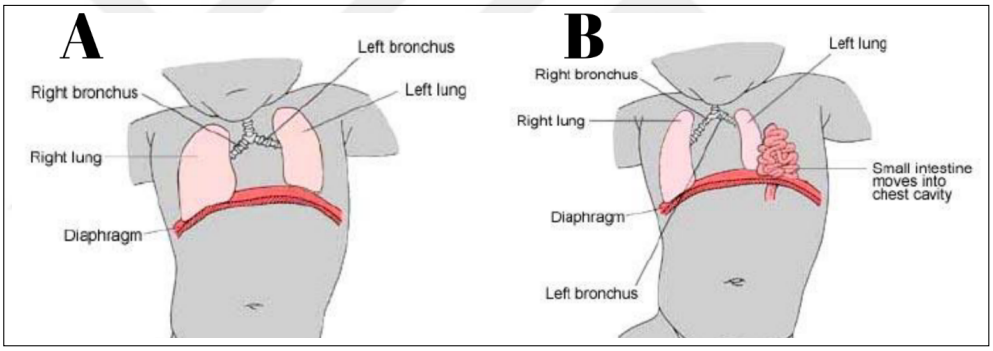

Figure 2.2 A: Normal chest cavity, B: Chest cavity with CDH [3].

2.2.1 Pulmonary Hypoplasia

Pulmonary hypoplasia is one of the main results of CDH. There are many hypotheses about its pathophysiology. The most widely accepted one is the double-hit theory. Herniation of the abdominal organs into the thorax is the result of the first hit that causes a defect in the diaphragm. The second hit results in hypoplastic lungs (Figure 2.3). Hence, a decrease in the low number of alveoli and airways is observed. Moreover, pulmonary hypoplasia may bring along heart diseases as well as respiratory disorders [30]. Pulmonary hypoplasia could be detected in cross-sectional imaging methods that will be discussed in the imaging methods of the CDH section. Current

medical technologies help both for diagnosis and treatment of pulmonary hypoplasia. After diagnosis and determining the severity of the anomaly, to provide a better respiratory system in the postnatal period, a minimally invasive method named fetal Tracheal Occlusion (TO) could be used, during which a balloon is placed endoscopically into the trachea and it helps the lungs to expand [31].

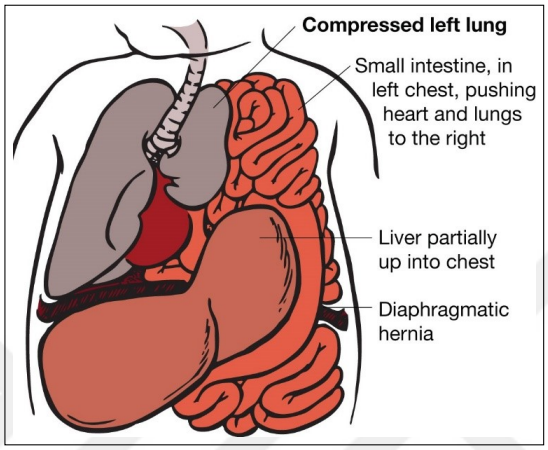

Figure 2.3 Pulmonary hypoplasia as consequence of CDH [4].

2.2.2 Pulmonary Hypertension

Pulmonary hypertension is another result of CDH that is caused by abnormal muscularization in arterioles [32]. It affects oxygenation and ventilation, and it causes high pressure in the pulmonary arteries after birth [33]. During the fetal period, the fetus gets the oxygenated blood from the mother through the umbilical cord. Thus, the effects of pulmonary hypertension could not be observed during the fetal period. The only possible but not feasible way to demonstrate pulmonary hypertension in utero is the histologic analysis of the lung by biopsy or during an autopsy. However, it is not only inappropriate to perform a biopsy in the fetus, but also the results may not apply to the whole lung. The vessel network of the lung has a key role both delivering the nutrients to the lung and its growth. Therefore, pulmonary hypertension is directly correlated with the pulmonary vasculature network of the lung.

2.3 Imaging Methods of Congenital Diaphragmatic Hernia

Assessing the volume of the lung, detecting the place of the hernia and organ movements due to CDH is critical to make predictions during the prenatal period. Imaging the CDH may help to acknowledge the parents and prepare them for the outcomes of this anomaly. Usually, the diagnosis time of CDH is approximately 16-24th week of gestation [34]. Detection failures may happen due to later occurrences on the diaphragm. With routine ultrasound imaging, anomaly could be detected by imaging the amniotic fluid of the fetus and organs that have gone up the diaphragm, but for certain analysis, more detailed ultrasound imaging and MR imaging techniques should be used to learn the severity of the disease.

2.3.1 Ultrasound Imaging

Using routine prenatal ultrasound imaging has increased the detection ratio of CDH. There are direct and indirect parameters to assess the severity of CDH. While the displacement of the abdominal organs is a direct sign, polyhydramnios, and abnormal cardiac axis or mediastinal shift are predictors that help to predict the presence of the anomaly [35]. By using ultrasound, it is easy to view the displacement of the organs due to the defect in the diaphragm, whereas the liver herniation, which is associated with poor prognosis, is difficult to detect per the echogenicity of the liver and lung are very close to each other [35]. Usually, the mortality risk could be determined by measuring the lung-to-head volume ratio [25].

2.3.2 Fetal Magnetic Resonance Imaging

Ultrasound imaging is frequently preferred due to its low cost, practical usage, and no harmful effects, but it may be inadequate in detecting some anomalies because it is not good at imaging soft tissues and it has lower resolution because of the amniotic fluid in the placenta. In these cases, in addition to ultrasound images, magnetic

resonance imaging (MRI) may be needed for a more accurate diagnosis. MRI provides high-resolution imaging of soft tissues that ultrasound could not display. MRI is applied in the 2nd or 3rd trimester of pregnancy. MR imaging is a more complicated technique, and the data acquisition time is longer compared to ultrasound imaging. Additionally, movement of the patient while imaging distorts the image, to prevent this distortion either fetal anesthesia is performed or there are new sequences in the MRI technologies. New MR sequences like single-shot fast-spin echo (SSFSE), also known as half-Fourier acquisition turbo spin-echo (HASTE), have been developed for fetus imaging which requires less acquisition time [5]. The data is received from the k-space by one RF excitation at a time that helps to overcome motion artifacts. However, it also results in a lower signal to noise ratio and lowers spatial resolution due to higher T2 decay at the longer echo trains [36].

By using fetal-MRI, liver position and lung volume could be measured to diagnose CDH severity better than ultrasound imaging. However, MRI techniques are more expensive and complex. (Figure 2.4) shows an example of an ultrasound and MR image of the fetal brain with agenesis of the corpus callosum. MR images could depict the lack of white matter connection while the ultrasound image couldn't show it.

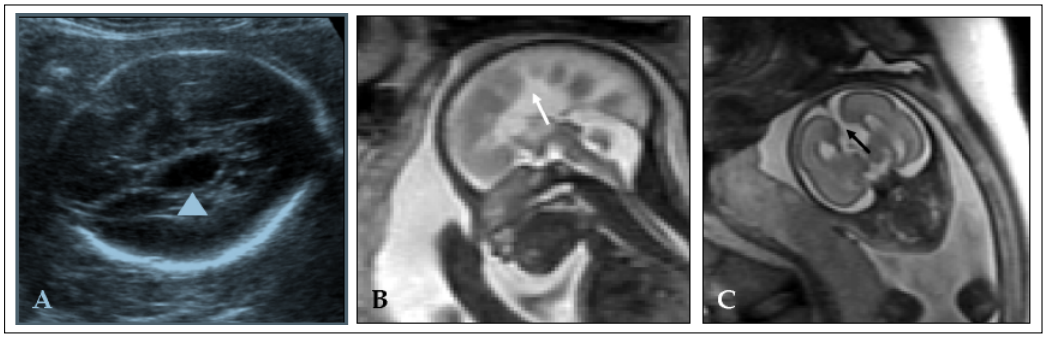

Figure 2.4 Comparison between ultrasound (A) and MRI (B, C) on the agenesis of the corpus callosum. MR images could depict the lack of connection of white matter, while ultrasound images couldn't show it [5].

2.3.3 Computed Tomography Imaging

In computed tomography imaging (CT), three-dimensional and cross-sectional images are provided by using the different attenuation characteristics of X-rays in different tissues. CT is a non-invasive imaging method and provides high-resolution images quickly, which makes CT scanners the workhorse of the radiology clinics. However, ionizing radiation effects of X-rays may have risks. Especially in pregnant women, CT is contraindicated due to its teratogenic effects. For this reason, fetal imaging by CT is not the desired option and is not recommended unless there is an emergency such as a shotgun injury in the abdomen.

The detection of CDH and follow-up of lung development could be performed by CT imaging in adults. As a result of the contrast agent injected into the pulmonary arteries, the lung vessels could be imaged in detail.

The use of CT in small animal subjects is carried out by micro-computed tomography (μCT) devices due to both cost concerns and size differences. μCT devices are less costly and provide a higher resolution on small animals such as mice and rats.

2.4 Literature Review

Due to high mortality and morbidity in CDH, there are many studies in the literature regarding its pathophysiology.

Many studies for the prenatal diagnosis of pulmonary hypoplasia have been done using different techniques. Currently, especially ultrasound and magnetic resonance imaging techniques are capable of detecting pulmonary hypoplasia easily. Various methods determining the effect of pulmonary hypoplasia on mortality and morbidity rates have taken place in the literature. The general belief is that fetuses with CDH that has a lung to head ratio (LHR) of less than 1 have a high postnatal mortality rate [8, 25, 37, 38]. However, there have been some studies like Arkovitz et al.'s [39] claiming

that LHR could not reliably be used to predict the outcomes of CDH. Other studies exist that have used place of liver herniation, gestational age, total lung volume ratio, and presence of polyhydramnios to make predictions on postnatal survival [9, 25, 40].

Pulmonary hypertension, which is another consequence of CDH, has a major effect on neonatal morbidity and mortality ratio. Although it is not possible to make a certain diagnosis in the prenatal period, there has been a study that made predictions about the severity of pulmonary hypoplasia [41]. Mahieu et al. [42] used a power doppler imaging method to show pulmonary arteries during the fetal period, but their study claimed that LHR was giving more accurate predictions.

3. MATERIALS and METHODS

3.1 Subjects

For this study, pregnant Sprague Dawley rats who have 22 days on term were harvested on the 21st day of gestation. To get chest images of the rats, a μCT scanner device (MicroCAT II) was used. To get a better visualization of the vascular system and exact structure of the vascular network, fetuses were put into lugol solution. By this new method, Aydin et al. achieved to diffuse lugol solution without damaging the vessels [20]. After the elimination of the low contrast and abnormal data, 15 healthy and 5 left-sided sick rat fetuses were obtained. The study protocol was approved by IACUC protocol 2016-0068 from Cincinnati Children's Research Foundation Institutional Animal Care and Use Committee.

3.2 Data Processing

Image processing techniques were applied using commercially available software (Analyze pro, Mayo Clinic). The chest data included parts that were not necessary for segmentation. An improved watershed algorithm was applied to the data to remove unwanted parts. The watershed algorithm did not apply to sick subjects due to distortions of the edges. The watershed algorithm is an image segmentation algorithm that is based on pixel intensities. As a drainage analogy, water flows down from high places and the path it follows is the watershed. The same approach could be applied in image segmentation. Higher and lower places correspond to the higher and lower pixel intensities. Hence, the edges of the partitions are watersheds, which makes it possible to segment [43].

A contrast agent was injected into the subjects to increase the visibility of the vessels. However, in some cases, the contrast agent didn't get distributed well or in

some points, distortions occurred. In order to obtain the appearance of the vessel network and to get rid of some low-level pixel intensities, a manual threshold was applied to each data. If the pixel value at a coordinate (i, j) was less than a threshold value, that pixel value was assigned to zero.

After determining the proper threshold manually, a semi-automated, pixel-based segmentation algorithm named as region growing was applied to the lung images. The region growing algorithm tracked the seeds that were put on the vessel points and formed the vessel structures. It simply checks the neighbor pixels and follows the network along a whole vessel [44]. This method is applicable when the pixel value distributions of the vessels are obviously different from other tissues. In some cases, due to the distortion of the contrast agent, the region growing method was not able to track the whole network. To overcome this issue, the threshold value was set to a low level, but this approach caused noise at the network structure. The noise was eliminated by manual segmentation. The segmented structure covered both arteries and veins. Since pulmonary hypertension affects the pulmonary arteries [45], it was necessary to evaluate pulmonary arteries only. So, arteries were manually separated from veins for the rat data.

To get morphometric measurements of the arteries like the number of branches, the average cross-sectional area, and the lengths of vessels, the skeletonization process was applied to the binary artery images by applying a thinning algorithm [46]. The thinning algorithm chose the center pixel and deleted neighbor pixels hence it kept the shape and structure of the object (Figure 3.1). After the skeletonization process, the tree structures of the arteries were obtained (Figure 3.2).

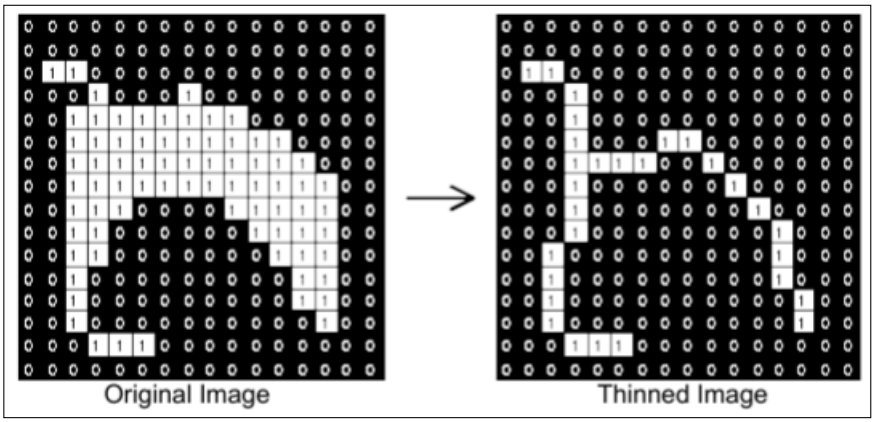

Figure 3.1 Thinning algorithm example [6].

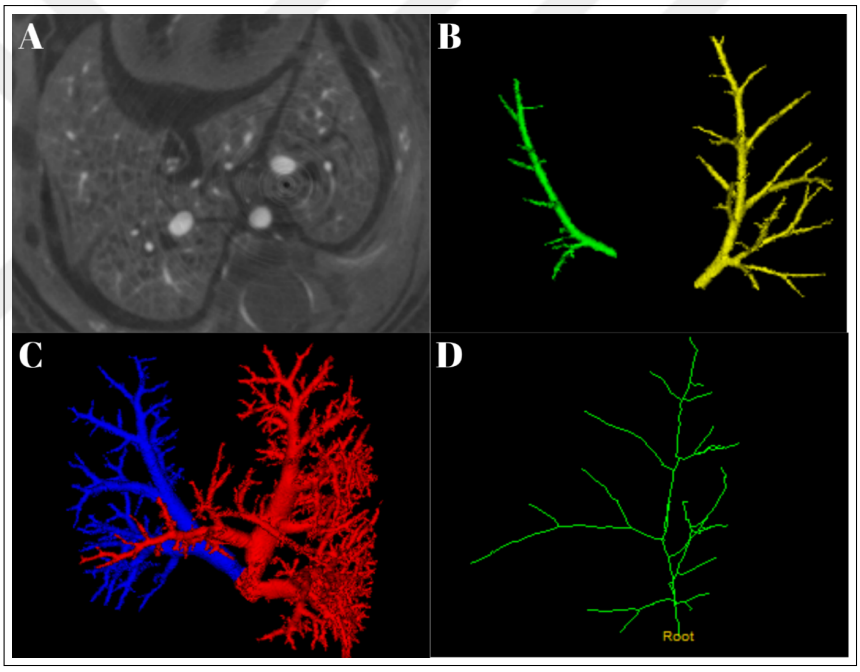

Figure 3.2 A: Cropped CT lung image, B: Segmented left and right arteries, C: Segmented left and right veins, D: Skeletonized right artery.

After skeletonized tree structures were available, the number of branches and branch generation information of the vessels was obtained. The root point was assigned manually to the tree structure at the beginning point of the artery. After the assignment of the root point was made, the first deviation point encountered in the tree structure was assigned as a new node (Figure 3.3).

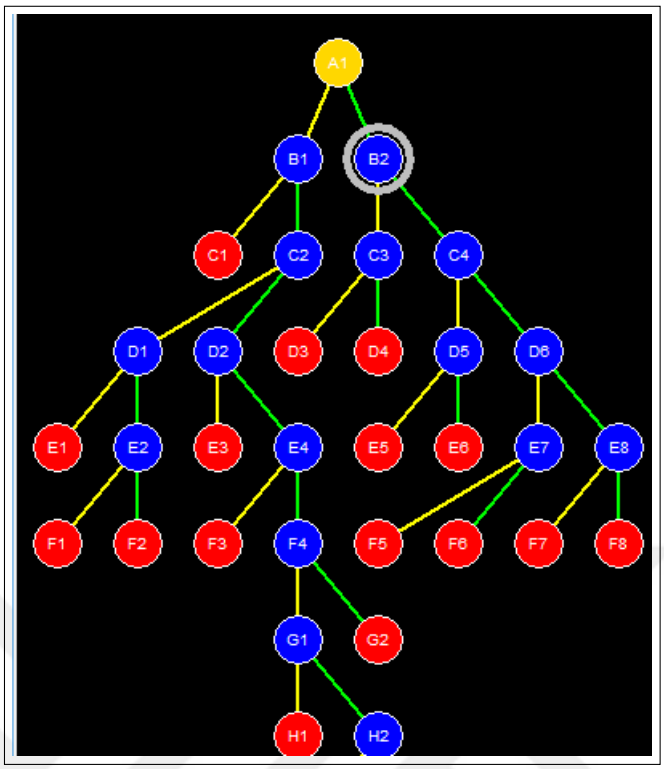

Figure 3.3 Generation map.

To get the area of the branches, binary structure, and skeletonized structures were rendered (Figure 3.4).

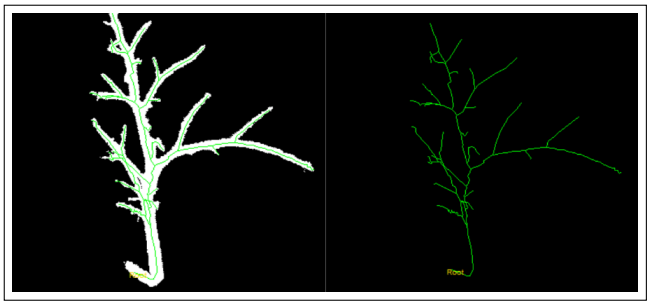

Figure 3.4 Rendered tree structure.

Subsequently, a radius value was determined, and for each node, and tree structure measurements were obtained (Figure 3.5). Each tree structure output was saved into a file for subsequent analysis.

Name	Area Product	BAP St Dev	Average Area	Area St Dev	Length	Children (Name,Angle)
A1	0.00	0.00	101.25	4.86	4	(B1, 142.6) (B2, 27.0)
B1	0.00	0.00	135.47	21.04	94	(C1, 131.8) (C2, 160.8)
C1	0.00	0.00	108.14	18.71	22	(D1, 170.0) (D2, 103.7)
D1	0.00	0.00	47.71	21.50	28	(E1, 133.3) (E2, 130.3)
E1	0.00	0.00	28.90	10.95	10	
E2	0.00	0.00	29.02	14.39	44	
D2	0.00	0.00	72.54	20.12	24	(E3, 151.7) (E4, 92.3)
E3	0.00	0.00	47.33	7.73	15	(F1, 119.8) (F2, 159.0)
F1	0.00	0.00	15.47	17.23	32	
F2	0.00	0.00	42.24	7.25	54	(G1, 142.2) (G2, 154.7)
G1	0.00	0.00	27.62	24.79	13	
G2	0.00	0.00	22.69	12.98	39	
E4	0.00	0.00	16.81	31.67	26	
C2	0.00	0.00	144.90	3.40	21	(D3, 108.6) (D4, 166.0)
D3	0.00	0.00	121.17	19.27	18	(E5, 124.2) (E6, 172.0)
E5	0.00	0.00	71.57	44.93	14	
E6	0.00	0.00	140.20	4.14	15	(F3, 168.5) (F4, 114.6)
F3	0.00	0.00	57.24	31.18	51	(G3, 105.9) (G4, 171.5)
G3	0.00	0.00	33.12	16.05	60	

Figure 3.5 An example of a tree structure measurement.

The comparison of arterial structures was conducted in two different ways. In the first method, the total arterial structures of the right and left lobes were compared. Parameters such as the length of the vessels, cross-sectional area, and the number of branches were obtained as shown in Figure 3.5. The other method was more detailed, and the right and left arteries were ordered according to their cross-sectional areas and a comparison was made between the orders of each lobe separately. When the root point was selected as the starting point of the artery, Analyze automatically assigns generation upwards to the node points. However, ordering generations in this way means that the diameters of the vessels were ignored, so comparisons may not give precise results. Jiang et al. [7] modified Strahler's stream order method as diameter defined Strahler system to order artery branches of the rats according to the size of their cross-sectional area. According to the stream order method of Strahler, the tributaries of the river are ordered according to their size. If two same orders merge, they form a higher-order branch, but if a larger and smaller branch merges, the degree is assigned to the larger one [47]. In diameter defined Strahler system, the part between the two bifurcations is called a segment. Serially aligned segments of the same order combine to form elements. It could be seen at the bottom of the right side of Figure 3.6 that two order two branches merge, but the next generation is still order two instead of

order three because this system considers diameters too.

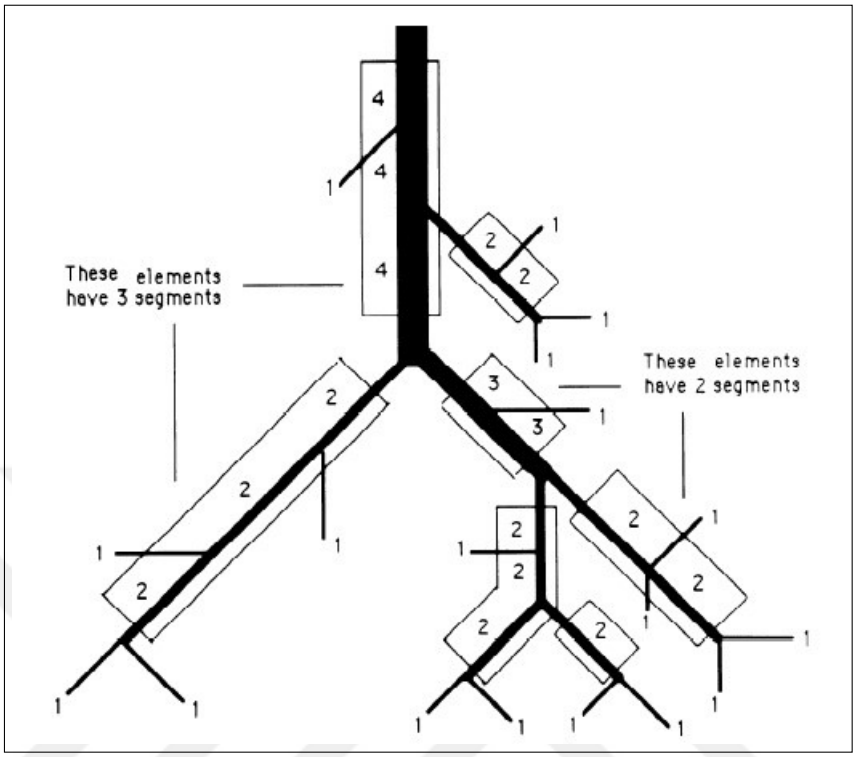

Figure 3.6 Diameter defined Strahler system [7].

The modified Strahler method was applied to our morphometric results and 4 orders were determined due to cross-sectional area values (Figure 3.7).

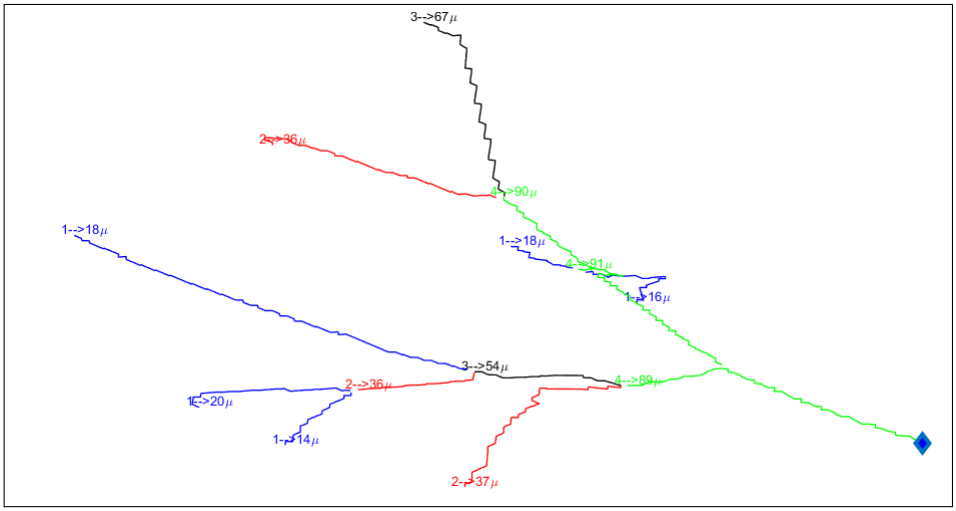

Figure 3.7 An example of an ordered artery branches.

3.3 Statistical Analysis

After data processing, the number of branches, the length of the vessels, and the average cross-sectional area of branches were obtained for total artery structure comparison. The right and left lobes were analyzed separately due to the placement of the anomaly by using a Mann-Whitney U test.

For ordered artery structure comparison, the number of branches, length of vessels, length to average cross-sectional area ratios, and connectivity matrices were computed in MATLAB (MathWorks Inc., Natick, MA). Control and the CDH groups were compared by using a Mann-Whitney U test for each order. The parameters of the right and left lobes of the healthy group were compared using a Wilcoxon signed-rank test. $P<=0.05$ was considered as statistically significant.

4. RESULTS

4.1 Comparison of the Total Networks

Table 4.1 shows the comparison of the morphometric results of the rat arterial networks. The parameters were evaluated separately for the left and right lobes of the control and the CDH groups. While the mean (±std) value of the vessels' cross-sectional area had no significant difference between healthy and sick subjects at the left lobe (P=0.43), it was lower in the control group at the right lobe (P=0.015). No statistically significant differences were observed between the vessel lengths of sick and healthy subjects for both lobes. The number of branches was lower in sick subjects than control subjects for both the left and right lobes (P<0.05).

Table 4.1
Comparison of the morphometric results of the lung vasculature and results of Mann-Whitney U test.

	Left			Right		
	Control (n=14)	CDH (n=5)	P-Value	Control (n=15)	CDH (n=5)	P-Value
Cross-Section Area	57.09±18.95	71.05±15.53	0.431	56.83±17.81	92.16±26.75	0.015
Vessel Length	32.02±6.17	40.42±13.84	0.817	35.32±3.57	30.05±9.56	0.727
Number of Branches	30.78±13.15	14.20±7.44	0.029	42.20±12.19	15.40±6.62	0.002

4.2 Comparison of the Ordered Artery Networks

The order of the arteries was determined according to their position in the arterial network, while taking into account the diameter of the vessels. Table 4.2 shows the range of vessel diameters for different arterial orders on the right and left lobes of the subjects.

Table 4.2
The range of vessel diameters for different arterial orders on the right and left lobes of the subjects.

Orders (n)	1	2	3	4
Range for Left Lobes (μm)	0-34.67	34.67-55.93	55.93-77.52	77.52-160.51
Range for Right Lobes (μm)	0-28.29	28.29-49.21	49.21-76.85	76.85-200.58

Table 4.3 shows the comparison of the number of branches. Statistically significant differences were observed between healthy and CDH subjects for both lobes. The number of branches was higher for control subjects than CDH subjects for order 1 and 2 on both right and left lobes ($P<0.05$ for all). However, for order 3, a statistical difference was observed only for the right lobe ($P=0.017$), and there was not a statistically significant difference for order 4. A comparison of the right and left lobes of the healthy rats revealed a significant difference only for order 2 ($P=0.007$).

Table 4.3
The comparisons of the number of branches for each order.

	Control		CDH		P-Values		
	Right	Left	Right	Left	Control-CDH (Right)	Control-CDH (Left)	Right/Left (Control)
Order 1	12.20±7.00	9.36±6.30	0.40±0.89	1.60±2.07	0.001	0.003	0.322
Order 2	13.00 ±5.32	8.00±3.40	4.40±2.97	4.40±1.67	0.006	0.032	0.007
Order 3	8.67±4.58	5.64±4.03	3.60±2.70	4.20±3.11	0.017	0.609	0.070
Order 4	8.33± 6.50	7.79± 6.33	6.20± 3.70	4.80±4.27	0.661	0.435	0.768

Table 4.4 shows the results of the comparison of the length of branches. A statistically significant difference was observed only for the right lobe of order 3 and CDH subjects had a lower length of branches than control subjects ($P=0.012$). The comparison of the right and left lobes of the healthy rats revealed a significant difference only for order 3 ($P=0.04$).

Table 4.5 shows the results of the length to diameter ratio (LDR) comparisons.

Statistically significant differences were observed for order 1 at the left lobe and order 2 at the right lobe. CDH subjects had a lower length to diameter ratio than control subjects for order 1 at the left lobe (P=0.004) and order 2 at the right lobe (P=0.029). Additionally, for the comparison of healthy rats' lobes, a difference was observed only for order 3 (P=0.012).

Table 4.4
The comparisons of the length of branches for each order.

	Control		CDH		P-Values		
	Right	Left	Right	Left	Control-CDH (Right)	Control-CDH (Left)	Right/Left (Control)
Order 1	45.03±35.19	39.33±21.04	88.74±32.56	28.51±13.96	0.062	0.165	0.476
Order 2	45.12±35.16	42.29±26.39	39.97±28.50	55.22±52.42	0.503	0.395	0.760
Order 3	39.90±35.35	29.28±23.65	52.29±30.60	34.43±37.95	0.012	0.905	0.047
Order 4	26.98±22.44	25.63±28.74	28.98±25.15	25.60±26.98	0.994	0.906	0.210

Table 4.5
The comparisons of the length to diameter ratios.

	Control		CDH		P-Values		
	Right	Left	Right	Left	Control-CDH (Right)	Control-CDH (Left)	Right/Left (Control)
Order 1	9.83± 3.19	8.47±2.22	15.17±0.00	4.35±3.60	0.053	0.004	0.125
Order 2	8.75±2.46	9.29±9.41	6.04±2.15	8.83±4.22	0.029	0.823	0.176
Order 3	7.06±3.74	5.04±1.84	8.37±4.36	4.93±3.45	0.662	0.753	0.012
Order 4	4.43±2.39	5.70±3.52	5.59±2.32	6.81±7.30	0.190	0.775	0.815

Table 4.6 and Table 4.7 are connectivity matrices of right and left lobes. The connectivity matrix results for both left and right lobes showed the connections between vessels of different orders. A connectivity matrix entry, C_{mn}, is the ratio of the total number of arteries with order m springing from order n to the total number of elements of order n. The number of the springing branch information was corrected by the diameter information as defined in the Strahler method. According to these connectivity matrix results, we observed that the connection numbers of generations

having small orders were reduced in CDH compared to healthy controls. The absence of a connectivity matrix value is an expected result for entries with an m of greater than n because the formation of large arteries from smaller arteries is not observed in vessel branching. Moreover, the value of an element C_{mn} was assumed to be 0 if the corresponding arterial tree did not have an element of order n.

Table 4.6
Connectivity matrix for right lobe.

	Control				CDH			
Orders	1	2	3	4	1	2	3	4
1	0.06±0.09	0.68±0.61	0.54±0.28	0.25±0.32	0	0.04±0.08	0.05±0.11	0
2	0	0.08±0.09	1.04±0.53	0.80±0.38	0	0.04±0.08	0.55±0.57	0.82±0.75
3	0	0	0.09±0.14	0.94±0.57	0	0	0	1.10±0.65
4	0	0	0	0.44±0.31	0	0	0	0.43±0.25

Table 4.7
Connectivity matrix for left lobe.

	Control				CDH			
Orders	1	2	3	4	1	2	3	4
1	0.06±0.08	1.13±1.37	0.76±0.39	0.40±0.44	0	0.07±0.15	0.20±0.45	0.30±0.48
2	0	0.04±0.11	0.94±0.76	1.13±0.60	0	0	0.89±0.63	0.60±0.30
3	0	0	0.03±0.06	1.03±0.49	0	0	0	1.10±0.66
4	0	0	0	0.39±0.31	0	0	0	0.23±0.29

5. DISCUSSION

CDH is an important factor in neonatal mortality today. Various studies on how the disease will affect the fetus in the prenatal period are generally based on evaluation of the total volume of the lung and its ratio to the body as a consequence of the pulmonary hypoplasia. Pulmonary hypertension, which is another consequence of CDH, should also be evaluated to increase the precision of predictions. In this study, we tried to determine the effects of pulmonary hypoplasia and pulmonary hypertension on pulmonary arteries on rat chest µCT images. Sick and healthy rat subjects were compared in terms of their morphometric parameters after the segmentation of the lung vasculature. As a result of this study, we determined that morphological changes were observed in the pulmonary arteries of the rats with CDH using noninvasive µCT imaging.

The comparison of the total vasculature networks was conducted to observe the overall change of arteries as a result of the CDH. It was observed that the average number of vessel branches of arteries was lower on both left and right sides as expected in rats with CDH. In previous studies, a decrease in the arborization of the pulmonary arteries was observed with invasive histological tissue analysis in different types of animal and human studies with CDH [13, 48, 49]. The main reason for this outcome is pulmonary hypoplasia, which prevents vascular branching [17]. Also, the fact that the contrast agent could not reach the ends of the arteries due to pulmonary hypoplasia, which prevents a complete visualization of these vessels, could be another factor. Hence, the visualized number of branches could be less than the actual number. While the mean value of the cross-sectional area of the vessels was high in sick rats in both right and left lobes, a statistically significant difference was observed only in the right lobe. Previous studies have shown that CDH causes the pulmonary artery to get muscular, and the internal diameter of the artery decreases while the external diameter of the artery expands [49, 50, 51]. Thinned internal artery diameter in both lobes is an expected result, but in our findings, no statistical difference was observed in the left

lobe. Additionally, the mean cross-sectional area is expected to be high due to the small arterioles that could not be displayed for the sick rats. Additionally, the organs herniated through the defect on the diaphragm that was present on the left side, and this applied pressure to the left lobe of the lungs, which prevented arborization. The vessel length is another parameter that was used in this study. No studies related to vessel length with pulmonary hypoplasia or pulmonary hypertension were found in the literature. Hypothetically, the effect of pulmonary hypoplasia on the length of the vessels in the sick subjects should be observed. However, there was no statistically significant difference between sick and healthy rats. This may be due to the fact that pulmonary hypoplasia does not affect the vascular length, but the limitations that we encountered during the vessel segmentation process may also have affected the results.

The parameters that were used in the comparison of the ordered arteries were the number of branches, length of branches, LDR, and connectivity matrices. While the number of branches was statistically different in small orders, the difference in the number of branches was not observed as the order number increased. Previous studies reported that CDH affected arterioles more, which is in agreement with our results [17, 48]. A difference in the vessel lengths was observed only in order 3. This result may be related to the fact that the arteries of order 3 were not properly imaged due to incomplete contrast agent diffusion. In agreement with the total comparison results, no statistically significant difference in vessel length was observed in ordered comparison. Additionally, the ratio of the lengths to the diameters was compared for each order. Internal artery diameters were expected to be thinner in subjects with CDH as reported in the previous studies [49, 50, 51]. However, a difference was only observed in order 1 of the left lobe and order 2 of the right lobe. This result may be related to the inability to visualize small arterioles in subjects with CDH. Moreover, the connectivity matrix results demonstrated that the connection numbers of generations having small orders were reduced in CDH compared to healthy controls. It could be seen that order 1 of the CDH group for both lobes didn't spring from bigger orders. This means that small arterial structures could not be visualized due to CDH, or small artery branching was prevented due to CDH, which was also previously reported [49].

In this study we had some limitations that may have impacted the results. First, some vessels which did not have a good contrast uptake were not properly visualized in some rat data, or there were disconnections between some vessel networks (Figure 5.1). Those data points had to be discarded. Hence, the amount of rat data was small at the end (healthy=15, CDH=5). With a larger dataset, more accurate results could be obtained. Additionally, the semi-automatic segmentation of lung vessels using Analyze (pro) program is a process that required quite an effort and time, and it might possible to do this process faster by using deep learning models. In order to increase effectivity of deep learning models, the data preprocessing stage is important. The segmentation of the vessels by using deep learning methods couldn't be applied in this study. However, we developed scripts to label the data in Python, which could later be used in the development of a deep learning model.

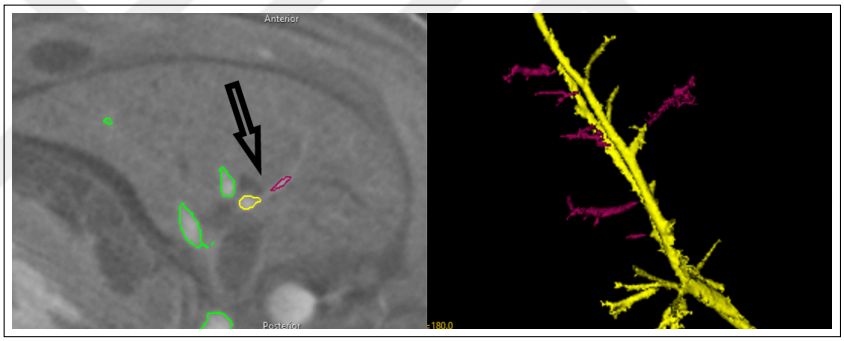

Figure 5.1 Vessel disconnection due to weak contrast.

.

6. CONCLUSION

In conclusion, the effects of CDH could be evaluated utilizing morphometric measurements of the pulmonary arteries besides the current methods, such as lung to head ratio, total lung volume, and right ventricle to the left ventricle ratio. The morphometric measures obtained as a result of this preliminary animal study could be translated into human studies. Since X-rays are dangerous for pregnant women and tomography is not recommended for imaging human fetuses, MRI will be employed for imaging human fetuses in future studies.

REFERENCES

1. Herbert, R. A., K. S. Janardhan, A. R. Pandiri, M. F. Cesta, V. Chen, and R. A. Miller, "Lung, Pleura, and Mediastinum," in *Boorman's Pathology of the Rat*, pp. 437–466, Elsevier, jan 2018.

2. "Lung Anatomy of a Human." Available: https://bit.ly/2ZS70Vv.

3. "Congenital Diaphragmatic Hernia Information Sheet for the Fetal Healthcare." Available: https://www.fetalhealthfoundation.org/fetal-syndromes/congenital-diaphragmatic-hernia/.

4. "Pulmonary Hypoplasia." Available: https://fetus.ucsf.edu/cdh.

5. Sohn, Y. S., M. J. Kim, J. Y. Kwon, Y. H. Kim, and Y. W. Park, "The usefulness of fetal MRI for prenatal diagnosis," *Yonsei Medical Journal*, Vol. 48, pp. 671–677, aug 2007.

6. "Thinning Algorithm." Available: https://homepages.inf.ed.ac.uk/rbf/HIPR2/thin.htm.

7. Jiang, Z. L., G. S. Kassab, and Y. C. Fung, "Diameter-defined Strahler system and connectivity matrix of the pulmonary arterial tree," *Journal of Applied Physiology*, Vol. 76, no. 2, pp. 882–892, 1994.

8. Bahlmann, F., E. Merz, C. Hallermann, H. Stopfkuchen, W. Krämer, and M. Hofmann, "Congenital diaphragmatic hernia: ultrasonic measurement of fetal lungs to predict pulmonary hypoplasia," *Ultrasound in Obstetrics and Gynecology*, Vol. 14, pp. 162–168, sep 1999.

9. Thébaud, B., A. Azancot, P. De Lagausie, E. Vuillard, L. Ferkadji, K. Benali, and F. Beaufils, "Congenital diaphragmatic hernia: Antenatal prognostic factors. Does cardiac ventricular disproportion in utero predict outcome and pulmonary hypoplasia?," *Intensive Care Medicine*, Vol. 23, no. 10, pp. 1062–1069, 1997.

10. Mahieu-Caputo, D., P. Sonigo, M. Dommergues, J. Fournet, J. Thalabard, C. Abarca, A. Benachi, F. Brunelle, and Y. Dumez, "Fetal lung volume measurement by magnetic resonance imaging in congenital diaphragmatic hernia," *BJOG: An International Journal of Obstetrics and Gynaecology*, Vol. 108, pp. 863–868, aug 2001.

11. Usui, N., H. Okuyama, T. Sawai, M. Kamiyama, S. Kamata, and M. Fukuzawa, "Relationship between L/T ratio and LHR in the prenatal assessment of pulmonary hypoplasia in congenital diaphragmatic hernia," *Pediatric Surgery International*, Vol. 23, pp. 971–976, oct 2007.

12. Lipshutz, G. S., C. T. Albanese, V. A. Feldstein, R. W. Jennings, H. T. Housley, R. Beech, J. A. Farrell, and M. R. Harrison, "Prospective analysis of lung-to-head ratio predicts survival for patients with prenatally diagnosed congenital diaphragmatic hernia," in *Journal of Pediatric Surgery*, Vol. 32, pp. 1634–1636, W.B. Saunders, nov 1997.

13. Adzick, N. S., M. R. Harrison, P. L. Glick, D. K. Nakayama, F. A. Manning, and A. A. DeLorimier, "Diaphragmatic hernia in the fetus: Prenatal diagnosis and outcome in 94 cases," *Journal of Pediatric Surgery*, Vol. 20, pp. 357–361, aug 1985.

14. Albanese, C. T., J. Lopoo, R. B. Goldstein, R. A. Filly, V. A. Feldstein, P. W. Calen, R. W. Jennings, J. A. Farrell, and M. R. Harrison, "Fetal liver position and perinatal outcome for congenital diaphragmatic hernia," *Prenatal Diagnosis*, Vol. 18, pp. 1138–1142, nov 1998.

15. Hedrick, M. H., J. M. Estes, K. M. Sullivan, J. F. Bealer, J. A. Kitterman, A. W. Flake, N. Scott Adzick, and M. R. Harrison, "Plug the lung until it grows (PLUG): A new method to treat congenital diaphragmatic hernia in utero," *Journal of Pediatric Surgery*, Vol. 29, pp. 612–617, may 1994.

16. Colvin, J., C. Bower, J. E. Dickinson, and J. Sokol, "Outcomes of congenital diaphragmatic hernia: A population-based study in Western Australia," *Pediatrics*, Vol. 116, pp. e356–e363, sep 2005.

17. Kitagawa, M., A. Hislop, E. A. Boyden, and L. Reid, "Lung hypoplasia in congenital diaphragmatic hernia a quantitative study of airway, artery, and alveolar development," *British Journal of Surgery*, Vol. 58, pp. 342–346, may 1971.

18. Aktas, Y. S., G. Diniz, R. Ortaç, and E. Ö. Aktas, "Pulmonary hypertension grading in the neonate: Pediatric autopsy series compared with etiology of lung disease," *Aegean Pathology Journal*, Vol. 1, pp. 76–80, 2004.

19. Cuevas Guamán, M., A. C. Akinkuotu, S. M. Cruz, P. A. Griffiths, S. E. Welty, T. C. Lee, and O. O. Olutoye, "Extracorporeal membrane oxygenation in premature infants with congenital diaphragmatic hernia," *ASAIO Journal*, Vol. 64, pp. e126–e129, sep 2018.

20. Aydın, E., B. Levy, M. Oria, H. Nachabe, F. Y. Lim, and J. L. Peiro, "Optimization of pulmonary vasculature tridimensional phenotyping in the rat fetus," *Scientific Reports*, Vol. 9, pp. 1–6, dec 2019.

21. Kiserud, T., "Physiology of the fetal circulation," *Seminars in Fetal and Neonatal Medicine*, Vol. 10, pp. 493–503, dec 2005.

22. Schneider, D. J., and J. W. Moore, "Patent ductus arteriosus," *Circulation*, Vol. 114, pp. 1873–1882, oct 2006.

23. Meyerholz, D. K., C. J. Suarez, S. M. Dintzis, and C. W. Frevert, "Respiratory system," in *Comparative Anatomy and Histology*, pp. 147–162, Elsevier, jan 2018.

24. Enns, G. M., V. A. Cox, R. B. Goldstein, D. L. Gibbs, M. R. Harrison, and M. Golabi, "Congenital diaphragmatic defects and associated syndromes, malformations, and chromosome anomalies: A retrospective study of 60 patients and literature review," *American Journal of Medical Genetics*, Vol. 79, pp. 215–225, sep 1998.

25. Metkus, A. P., R. A. Filly, M. D. Stringer, M. R. Harrison, and N. S. Adzick, "Sonographic predictors of survival in fetal diaphragmatic hernia," in *Journal of Pediatric Surgery*, Vol. 31, pp. 148–152, W.B. Saunders, 1996.

26. Van Den Hout, L., T. Schaible, T. E. Cohen-Overbeek, W. Hop, J. Siemer, K. Van De Ven, L. Wessel, D. Tibboel, and I. Reiss, "Actual outcome in infants with congenital diaphragmatic hernia: The role of a standardized postnatal treatment protocol," *Early Human Development*, Vol. 29, pp. 55–63, feb 2011.

27. Torfs, C. P., C. J. Curry, T. F. Bateson, and L. H. Honoré, "A population based study of congenital diaphragmatic hernia," *Teratology*, Vol. 46, pp. 555–565, dec 1992.

28. Glick, P. L., J. R. Siebert, and D. R. Benjamin, "Pathophysiology of congenital diaphragmatic hernia: Renal enlargement suggests feedback modulation by pulmonary derived renotropins," *Journal of Pediatric Surgery*, Vol. 25, pp. 492–495, may 1990.

29. Lingman, G., and K. Maršal, "Fetal central blood circulation in the third trimester of normal pregnancy - a longitudinal study.," *Early Human Development*, Vol. 13, pp. 137–150, apr 1986.

30. Akinkuotu, A. C., F. Sheikh, D. L. Cass, I. J. Zamora, T. C. Lee, C. I. Cassady, A. R. Mehollin-Ray, J. L. Williams, R. Ruano, S. E. Welty, and O. O. Olutoye, "Are all pulmonary hypoplasias the same? A comparison of pulmonary outcomes in neonates with congenital diaphragmatic hernia, omphalocele and congenital lung malformation," *Journal of Pediatric Surgery*, Vol. 50, no. 1, pp. 55–59, 2015.

31. Deprest, J., E. Gratacos, and K. H. Nicolaides, "Fetoscopic tracheal occlusion (FETO) for severe congenital diaphragmatic hernia: Evolution of a technique and preliminary results," *Ultrasound in Obstetrics and Gynecology*, Vol. 24, no. 2, pp. 121–126, 2004.

32. Taira, Y., T. Yamataka, E. Miyazaki, and P. Puri, "Comparison of the pulmonary vasculature in newborns and stillborns with congenital diaphragmatic hernia," *Pediatric Surgery International*, Vol. 14, no. 1-2, pp. 30–35, 1998.

33. Iocono, J. A., R. E. Cilley, D. T. Mauger, T. M. Krummel, and P. W. Dillon, "Postnatal pulmonary hypertension after repair of congenital diaphragmatic hernia: Predicting risk and outcome," *Journal of Pediatric Surgery*, Vol. 34, no. 2, pp. 349–353, 1999.

34. Taylor, G. A., O. M. Atalabi, and J. A. Estroff, "Imaging of congenital diaphragmatic hernias," *Pediatric Radiology*, Vol. 39, no. 1, pp. 1–16, 2009.

35. Graham, G., and P. C. Devine, "Antenatal diagnosis of congenital diaphragmatic hernia," *Seminars in Perinatology*, Vol. 29, no. 2, pp. 69–76, 2005.

36. Loening, A. M., M. Saranathan, N. Ruangwattanapaisarn, D. V. Litwiller, A. Shimakawa, and S. S. Vasanawala, "Increased speed and image quality in single-shot fast spin echo imaging via variable refocusing flip angles," *Journal of Magnetic Resonance Imaging*, Vol. 42, pp. 1747–1758, dec 2015.

37. Deprest, J., J. Jani, D. Van Schoubroeck, M. Cannie, D. Gallot, S. Dymarkowski, J. P. Fryns, G. Naulaers, E. Gratacos, and K. Nicolaides, "Current consequences of prenatal diagnosis of congenital diaphragmatic hernia," *Journal of Pediatric Surgery*, Vol. 41, pp. 423–430, feb 2006.

38. Laudy, J. A., M. Van Gucht, M. F. Van Dooren, J. W. Wladimiroff, and D. Tibboel, "Congenital diaphragmatic hernia: An evaluation of the prognostic value of the lung-to-head ratio and other prenatal parameters," *Prenatal Diagnosis*, Vol. 23, pp. 634–639, aug 2003.

39. Arkovitz, M. S., M. Russo, P. Devine, N. Budhorick, and C. J. Stolar, "Fetal lung-head ratio is not related to outcome for antenatal diagnosed congenital diaphragmatic hernia," *Journal of Pediatric Surgery*, Vol. 42, pp. 107–111, jan 2007.

40. Datin-Dorriere, V., S. Rouzies, P. Taupin, E. Walter-Nicolet, A. Benachi, P. Sonigo, and D. Mitanchez, "Prenatal prognosis in isolated congenital diaphragmatic hernia," *American Journal of Obstetrics and Gynecology*, Vol. 198, pp. 80.e1–80.e5, jan 2008.

41. Spaggiari, E., J. J. Stirnemann, P. Sonigo, N. Khen-Dunlop, L. De Saint Blanquat, and Y. Ville, "Prenatal prediction of pulmonary arterial hypertension in congenital diaphragmatic hernia," *Ultrasound in Obstetrics and Gynecology*, Vol. 45, pp. 572–577, may 2015.

42. Mahieu-Caputo, D., M. C. Aubry, M. El Sayed, L. Joubin, J. C. Thalabard, and M. Dommergues, "Evaluation of fetal pulmonary vasculature by power doppler imaging in congenital diaphragmatic hernia," *Journal of Ultrasound in Medicine*, Vol. 23, pp. 1011–1017, aug 2004.

43. Ong, S. H., K. W. C. Foong, P.-S. Goh, W. L. Nowinski, H. P. Ng, S. H. Ong, K. W. C. Foong, P. S. Goh, and W. L. Nowinski, "Medical image segmentation using K-Means clustering and improved watershed algorithm," *2006 IEEE Southwest Symposium on Image Analysis and Interpretation*, no. February 2001, 2001.

44. Adams, R., and L. Bischof, "Seeded region growing," *IEEE Transactions on Pattern Analysis and Machine Intelligence*, Vol. 16, no. 6, pp. 641–647, 1994.

45. Ruano, R., M. C. Aubry, B. Barthe, D. Mitanchez, Y. Dumez, and A. Benachi, "Predicting perinatal outcome in isolated congenital diaphragmatic hernia using fetal pulmonary artery diameters," *Journal of Pediatric Surgery*, Vol. 43, no. 4, pp. 606–611, 2008.

46. Lobregt, S., P. W. Verbeek, and F. C. Groen, "Three-dimensional skeletonization: principle and algorithm," *IEEE Transactions on Pattern Analysis and Machine Intelligence*, Vol. PAMI-2, no. 1, pp. 75–77, 1980.

47. Strahler, A. N., "Quantitative analysis of watershed geomorphology," *Eos, Transactions American Geophysical Union*, Vol. 38, pp. 913–920, dec 1957.

48. DiFiore, J. W., D. O. Fauza, R. Slavin, C. A. Peters, J. C. Fackler, and J. M. Wilson, "Experimental fetal tracheal ligation reverses the structural and physiological effects of pulmonary hypoplasia in congenital diaphragmatic hernia," *Journal of Pediatric Surgery*, Vol. 29, no. 2, pp. 248–257, 1994.

49. Danzer, E., M. G. Davey, P. A. Kreiger, E. D. Ruchelli, M. P. Johnson, N. S. Adzick, A. W. Flake, and H. L. Hedrick, "Fetal tracheal occlusion for severe congenital diaphragmatic hernia in humans: a morphometric study of lung parenchyma and muscularization of pulmonary arterioles," *Journal of Pediatric Surgery*, Vol. 43, pp. 1767–1775, oct 2008.

50. Kanai, M., Y. Kitano, D. Von Allmen, P. Davies, N. S. Adzick, and A. W. Flake, "Fetal tracheal occlusion in the rat model of nitrofen-induced congenital diaphragmatic hernia: tracheal occlusion reverses the arterial structural abnormality," *Journal of Pediatric Surgery*, Vol. 36, pp. 839–845, jun 2001.

51. Lipsett, J., J. C. Cool, S. I. Runciman, W. D. Ford, J. D. Kennedy, and A. J. Martin, "Effect of antenatal tracheal occlusion on lung development in the sheep model of congenital diaphragmatic hernia: a morphometric analysis of pulmonary structure and maturity," *Pediatric Pulmonology*, Vol. 25, pp. 257–269, apr 1998.